environmental sciences proceedings

MDPI

Proceeding paper

Debris Flow and Flood Susceptibility Using Remote Sensing and GIS data: A Case of the Central Andes of Chile (33°13′ - 33°30′) †

Waldo Pérez-Martínez [1,2,*], Benjamín Castro-Cancino [1], Natalia Tapia-Pineda [1], Paulina Vidal-Páez [1,2], Idania Briceño-De-Urbaneja [1,2] and Freddy A. Saavedra [3,4,5]

[1] Hémera Centro de Observación de la Tierra, Facultad de Ciencias, Ingeniería y Tecnología, Universidad Mayor, Santiago 8580745, Chile; benjamin.castroc@mayor.cl, natalia.tapia01@mayor, paulina.vidal@umayor.cl, idania.briceno@umayor.cl
[2] Departamento de Ingeniería cartográfica, Geodesia y Fotogrametría, Universitat Politècnica de València, Valencia 46022, Spain
[3] Departamento de Ciencias Geográficas, Facultad de Ciencias Naturales y Exactas, Universidad de Playa Ancha, Valparaíso 2360002, Chile; freddy.saavedra@upla.cl
[4] Laboratorio de Teledetección Ambiental (TeleAmb), Universidad de Playa Ancha, Valparaíso 2360002, Chile
[5] HUB-AMBIENTAL UPLA, Universidad de Playa Ancha, Valparaíso 2360002, Chile
* Correspondence: waldo.perez@umayor.cl
† Presented at the 5th International Electronic Conference on Remote Sensing, 7–21 Nov 2023, available online at: https://ecrs2023.sciforum.net/ .

Abstract: In the study area, landslides represent the most frequent geological-geomorphological hazard in mountain environments, causing damage to infrastructure, local economies and loss of human lives. A landslide susceptibility map was developed, based on the sum of the weighted scores of the landslides conditioning factors. 21% of the study area is in high and very high susceptibility zones to be affected by landslides. These areas are concentrated in the headwaters of basins, valley bottoms, steep slopes and in the main riverbeds and streams.

Keywords: susceptibility; debris flow; debris flood; landslides; GIS; remote sensing; Santiago; Andes centrales Chile

1. Introduction

Landslide processes are defined as rapid or slow movements of rock, soil or both, of a gravitational nature [1], and are classified according to the type of material, movement, degree of soil saturation, among others; in rockfall, overturning, rotational or translational landslides, lateral spreading, creeping, debris flows and floods [1]. The occurrence of these phenomena is conditioned by factors such as lithology, geomorphology, structures, hydrology, hydrogeology, vegetation and climate; factors that trigger them include hydrometeorological, seismic and volcanic events [2].

In mountain environments, gravitational, snow, glacial, periglacial and fluvial processes interact [3], where slope, relief and extreme precipitation events increase the intensity of denudation and deposition processes [3]. Landslides are one of the most common phenomena of denudation or erosion of the topography in mountain environments, specifically, rotational or translational landslides, rock falls, debris flows and floods.

The Andes mountain range is characterized by its geological, geomorphological, tectonic and climatic conditions, in an area highly susceptible to the generation of different types of landslides [4]. Landslides are common in the Andean foothills and in the interior ravines of the basins, especially debris flows and floods that can reach the alluvial plains [5], which implies a risk for the population, increased by the sustained growth of cities

Citation: To be added by editorial staff during production.

Academic Editor: Firstname Lastname

Published: date

towards the foothills. This study contributes to the knowledge of areas susceptible to debris flow in the upper Mapocho river basin (33°13' - 33°30'), which includes the northeastern urban sector of the city of Santiago in the Andean foothills and the headwaters of the basin in the Andes mountain range, where tourism and mining activities are developed.

2. Material and Methods

2.1. Study Area

The study area has an extension of 1,021 km² and is located in the northeastern sector of the Metropolitan Region, in the upper Mapocho River basin, between coordinates 33°06'S - 33°29'S and 70°36'W - 70°11'. It is composed of the sub-basins of the Mapocho River between Estero Arrayán and Estero de Las Rosas; Estero Arrayán; San Francisco River and Molina River, which are part of the northeastern sector of the Maipo River basin (Figure 1).

The central zone of Chile is characterized by an interannual variability of precipitation, with an annual average between 100 and 2000 mm [6], produced by cold fronts, mostly concentrated in winter [6], and within a Mediterranean climate [6].

Geologically, it is composed of a group of volcanic, volcanoclastic and continental sedimentary rocks corresponding to the Abanico Formation (Upper Eocene-Lower Miocene) [7]. Through angular unconformity, overlies clastic, epliclastic and volcanic rocks of the Miocene volcanic arc, corresponding to the Farellones Formation (Lower Miocene - Upper Miocene) [7].

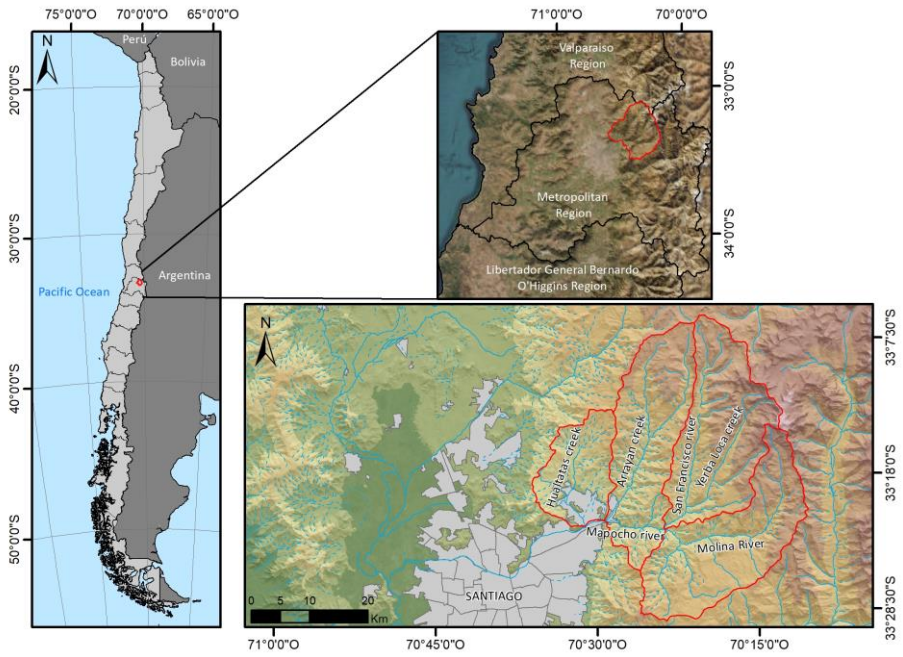

Figure 1. Location map of the study area. The main sub-basins and the rivers and creeks that compose them are shown.

2.2. Data Sources

A bibliographic and cartographic review of the geomorphology, hydrography, geology and land cover components was conducted. For the geomorphological, hydrographic and geological characterization, we used as a basis the photointerpretation of the Pléiades satellite image mosaic of 50 cm resolution (2015) and PlanetScope of 3 m resolution (2023); digital cartography of the Metropolitan Region, section E, scale 1:50,000; inventory of glaciers and water resources of the General Directorate of Water (2022); and DEM ALOS PALSAR 12.5 m resolution (2011), downloaded from server https://www.asf.alaska.edu/sardata/palsar/.

The forestation information layers and the persistence of snow cover were obtained from the time series analysis of Landsat and MODIS satellite images (2000-2022). The forestation data were downloaded from the server https://glad.earthengine.app/view/global-forest-change and snow cover persistence was elaborated and updated by [8]. Land uses were extracted from Castastro y Evaluacion de los Recursos Vegetacionales Nativos de Chile (2013) (Cadastre and Evaluation of Native Plant Resources of Chile) and downloaded from the server http://sit.conaf.cl/.

2.3. Conditioning Factors

A total of 14 conditioning factors were considered for the calculation of the Susceptibility Index (SI), associated to three groups, used by [9], and described below.

Slope gradient: The slope was calculated using the 12.5 m resolution DEM ALOS PALSAR, which was also used to calculate the slope orientation, profile curvature, topographic wetness index and drainage network hierarchy factors.

Solpe orientation: The orientation of the slopes when exposed to the sun influences melting and humidity processes, generating effects on erosive processes and material weathering, in addition to reducing the presence of vegetation due to the dryness of the area [10].

Profile curvature: Concave slopes with active erosion are considered more susceptible, while convex slopes have a lower susceptibility index [11].

Distance to geoforms: The geoforms correspond to linear elements of the surface and are related to higher degrees of fracturing, so neighboring zones are classified as having higher susceptibility [9].

Drainage network density: The number of drains in a surface unit of 1,000 m x 1,000 m was considered. The higher the drainage density, the higher the susceptibility and the lower the drainage density, the lower the susceptibility.

Distance drainage network by hierarchy: The drainage network conditions the permeability, saturation and filtration capacity of the soil, affecting the stability of the substrate, eroding and saturating the lower parts of the slopes [12]. The distances were defined according to the runoff and order of the drains.

Topographic Wetness Index (TWI): This index reflects the tendency of water to accumulate in areas of the basin [13]. An increase in this index is related to areas that are more prone to have landslide processes.

Geological units: Lithological units were determined from literature and cartographic review; and were reclassified based on the categories used by [14].

Fault density: Faults identified on geologic charts and maps are related to the decrease in rock strength [15]. To determine the fault density, observed and inferred faults were considered in a 1,000 m x 1,000 m grid.

Distance to faults: Areas close to faults are more prone to generate landslides than more distant areas [15]. Differentiated distances were considered for observed and inferred faults, attributing greater importance to observed faults.

Distance to folds: Similar to the criterion used for the distance to faults, the fold axis corresponds to a zone of increased weakness due to the development of associated fractures [9]. Susceptibility indexes were assigned according to the increase in distance to the fold axis.

Forest change: The map characterizing the extent and changes in forests during the period 2000-2022, developed by [16], was used, and categories of increase, stable and deforestation were established.

Land cover: A simplification of land uses from the Catastro y Evaluación de los Recursos Vegetacionales Nativos de Chile, a scale of 1:50,000 (2013) was used.

Snow persistence Elaborated and updated by [8], the Snow Cover Index (SCI) was considered, representing the snow frequency over 23 years (2000-2022) and at a percentage scale of 0-100%.

2.4. Susceptibility

Susceptibility is associated with the probability of landslides in a specific area due to local environmental conditions [17]. It was evaluated using a qualitative combination methodology of thematic maps [4,6,10,14,18]. It was quantified by calculating a Susceptibility Index (SI), which involves the sum of weighted scores for each one of the 14 conditioning factors considered in the study area [4,10,14] (Equation 1).

$$\mathrm{SI} = \sum_{i=0}^{14} f_i * map\ factor_i \quad (1)$$

Where f_i corresponds to each one of 14 conditioning factors reclassified in values between 0 and 5, where 0 indicates a factor that does not increase susceptibility and 5 indicates a factor that strongly influences susceptibility; and $map\ factor_i$ corresponds to the percentage assigned to each of the conditioning factors according to their level of importance and on a percentage scale of 0-100% (Table A1).

The initial weights considered were modified based on the work done by [9], then the percentage assigned to each of the conditioning factors according to their level of importance was determined using the Analytical Hierarchical Process (AHP), which considers a comparison of the contribution of the different factors in a pairwise matrix. To obtain the weights of the factors in the AHP, the methodology used by [19] was applied, where the construction of the pairwise comparison matrix implied that each factor was rated against each one of the other factors by assigning a relative dominant value between 1 and 9 in the intersection cell, considering the preference scale developed by [20]. Finally, the values obtained from the AHP was converted to a percent, where the sum of the 14 conditioning factor is 100%.

Table A1. Conditioning factors used to determine susceptibility [9].

Group	Subgroup	Percent
Geomorphology	Topography Geoforms	54%
Geology	Drainage Units Structures	34%
Soil condition	Forestation Coverage Snow	12%

ArcGIS® software was used to process the acquired data, create the new data, reclassify the thematic maps, calculate and categorize the SI using the Raster Calculator tool and Natural Breaks [21], to group similar values and determine the optimal number of categories (Table 2).

Table 2. Reclassification of the Susceptibility Index.

Susceptibility Index	Susceptibility
< 1.64	Very Low
1.64 – 1.94	Low
1.94 – 2.32	Moderate
2.32 – 2.75	High
> 3.86	Very High

3. Results

Based on 14 conditioning factors, a map of debris flow and flood susceptibility in the upper Mapocho river basin was generated, as shown in Table 3 and Figure 2.

Table 3. Area and percentage of susceptibility categories.

Susceptibility	Area (km²)	Percent
Very Low	201.93	19.81%
Low	358.14	35.14%
Moderate	237.81	23.33%
High	121.06	11.88%
Very High	100.29	9.84%

78.28% of the study area is located in areas of very low to moderate susceptibility to generate and be affected by flow and flood debris. The main zones with high and very high susceptibility to generate flow and flood debris, which correspond to 21.72% of the study area, are located mainly to the northeast of the basin headwaters, in the valley bottoms, on slopes with gradients greater than 20° and in geological units with a low degree of consolidation (alluvial, colluvial, fluvial and landslide deposits, glaciers, wetlands, lakes and sectors with mining activity).

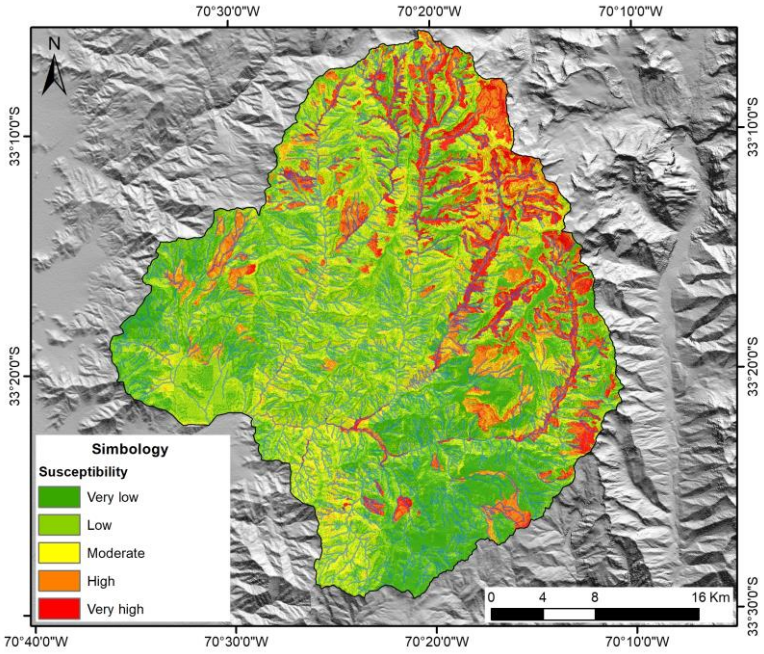

Figure 2. Debris flow and flood susceptibility map in the upper Mapocho river basin.

4. Conclusions

During the last decades, the foothills and highlands of the Metropolitan Region have had several landslide events. The events have been triggered mainly by climatic anomalies, torrential rains and, to a lesser extent, by earthquakes of varying intensity.

In the study area, the zones with the greatest susceptibility to be affected by debris flow and flood are concentrated in the main riverbeds and streams. This is consistent with the main types of landslide deposits recognized in the area, most of which correspond to hydric flows (with various concentrations of debris and water), which means that their mobility is essentially conditioned by topography.

A landslide susceptibility map, based on remote sensing data, digital mapping and GIS tools, is an effective tool for landslide monitoring, land use planning, generation of early warning systems and emergency plans to protect the population and infrastructure.

Author Contributions: Conceptualization, W.P.-M. and B.C.-C.; methodology, W.P.-M., P.V.-P., I.B.De-U.; software, B.C.-C., N.T.-P. and F.A.S.; validation, B.C.-C. and N.T.-P.; formal analysis, W.P.-M., B.C.-C. and N.T.-P.; investigation, W.P.-M., P.V.-P., I.B.De-U. and F.A.S.; resources, W.P.-

M.; data curation, B.C.-C., N.T.-P. and F.A.S.; writing—original draft preparation, W.P.-M. and B.C.-C.; writing—review and editing, W.P.-M. and B.C.-C.; visualization, B.C.-C.; supervision, W.P.-M. and B.C.-C.; project administration, W.P.-M.; funding acquisition, W.P.-M.

Funding: This research was funded by Hémera Centro de Observación de la Tierra of Universidad Mayor.

Acknowledgments: This study was supported by the Hémera Centro de Observación de la Tierra of Universidad Mayor, mining company Anglo American S.A. and is part of the doctoral thesis in Geomatics Engineering of the Universitat Politècnica de València, Spain.

Conflicts of Interest: The authors declare no conflict of interest.

Appendix A

Table A1. Weight and percentage of conditioning factors to determine susceptibility [9].

References

1. Hungr, O.; Leroueil, S.; Picarelli, L. The Varnes classification of landslide types, an update. *Landslides* **2014**, *11(2)*, 167-194. doi: 10.1007/s10346-013-0436-y.
2. Sepúlveda, S.A.; Moreiras, S.M.; Lara, M.; Alfaro, A. Debris flows in the Andean ranges of central Chile and Argentina triggered by 2013 summer storms: characteristics and consequences. *Landslides* **2015**, *12*, 115-133. doi:10.1007/s10346-014-0539-0.
3. Lambiel, C.; Maillard, B.; Kummert, M.; Reynard, E. Geomorphology of the hérens valley (Swiss alps). *J. Maps* **2016**, *12(1)*, 160–172. doi:10.1080/17445647.2014.999135.
4. Lara, M. & Sepúlveda, S.A. Landslide susceptibility and hazard assessment in San Ramón Ravine, Santiago de Chile, from an engineering geological approach. *Environ. Earth Sci.* **2010**, *60(6)*, 1227-1243. doi:10.1007/s12665-009-0264-5.
5. Lara, M.; Sepúlveda, S.A.; Celis, C.; Rebolledo, S.; Ceballos, P. Landslide susceptibility maps of Santiago city Andean foothills, Chile. *Andean Geol.* **2018**, *45(3)*, 433-442. doi:10.5027/andgeoV45n3-3151.
6. Viale, M., & Garreaud, R. Orographic effects of the subtropical and extratropical Andes on upwind precipitating clouds: effects of the Andes on precipitation. *J. Geophys. Res. Atmos.* **2015**, *120(10)*, 4962–4974. doi:10.1002/2014jd023014.
7. Muñoz-Sáez, C.; Pinto, L.; Charrier, R.; Nalpas, T. Influence of depositional load on the development of a shortcut fault system during the inversión of an extensional basin: The Eocene - Oligocene Abanico Basin case, central Chile Andes (33°-35°S). *Andean Geol.* **2014**, *41(1)*, 1-28. doi:10.5027/andgeoV41n1-a01.
8. Saavedra, F.A.; Kampf, S.K.; Fassnacht, S.R.; Sibold, J.S. Changes in Andes snow cover from MODIS data, 2000–2016. *The Cryosphere* **2018**, *12*, 1027–1046. doi:10.5194/tc-12-1027-2018.
9. Droguett, B.; Vidal-Páez, P.; Clavero, J.; Pérez-Martínez, W.; Briceño-De-Urbaneja, I.; Ramírez, V.; Tamayo, A. Heavy rain-induced debris flow/flood hazards at a geomorphologically active Andean valley: the case of the Yerba Loca basin, Central Chile. *Andean Geol.* **2023**. (review paper).
10. Lara, M. Metodología para la evaluación y zonificación de peligro de remociones en masa con aplicación en Quebrada San Ramón, Santiago Oriente, Región Metropolitana. Tesis para optar el grado de Magister en Ciencias, Mención Geología, Universidad de Chile, Departamento de Geología: 229 pp. 2007.
11. Wubalem, A. Landslide susceptibility mapping using statistical methods in Uatzau catchment area, northwestern Ethiopia. *Geoenviron. Disasters* **2021**, *8*. doi:10.1186/s40677-020-00170-y.
12. Nohani, E.; Moharrami, M.; Sharafi, S.; Khosravi, K.; Pradhan, B.; Pham, B.T.; Lee, S.; M.; Melesse, A. Landslide Susceptibility Mapping Using Different GIS-Based Bivariate Models. *Water* **2019**, *11*, 1402. doi:10.3390/w11071402.
13. Regmi, A.D.; Devkota, K.C.; Yoshida, K.; Pradhan, B.; Pourghasemi, H.R.; Kumamoto, T.; Akgun, A. Application of frequency ratio, statistical index, and weights of evidence model sand their comparison in landslide susceptibility mapping in Central Nepal Himalaya. *Arab. J. Geosci.* **2014**, *7(2)*, 725–742. doi:10.1007/s12517-012-0807-z.
14. Pérez-Martínez, W.; Pardo-Pascual, J.E.; Briceño, I.; Vidal, P. Study of Natural Hazards in the Upper Part of the Mapocho River Basin, Metropolitan Region of Chile, Using Satellite Imagery. *Proceedings* **2019**, *19*, 4. doi:10.3390/proceedings2019019004.
15. Abedin, J.; Rabby, Y.W.; Hasan, I.; Akter, H. An investigation of the characteristics, causes, and consequences of June 13, 2017, landslides in Rangamati District Bangladesh. *Geoenviron. Disasters* **2020**, *7*, 23. doi:10.1186/s40677-020-00161-z.
16. Hansen, M.C.; Potapov, P.V.; Moore, R.; Hancher, M.; Turubanova, S.A.; Tyukavina, A.; Thau, D.; Stehman, S.V.; Goetz, S.J.; Loveland, T.R.; Kommareddy, A.; Egorov, A.; Chini, L.; Justice, C.o.; Townshend, R.G. High-Resolution Global Maps of 21st-Century Forest Cover Change. *Science* **2013,** *342*, 850-853. doi:10.1126/science.1244693.
17. Aleotti, P.; Chowdhury, R. Landslide hazard assessment: summary review and new perspectives. *Bulletin of Engineering Geology and the Environment* **1999**, *58*, 21–44. doi:10.1007/s100640050066.
18. Vidal-Páez, P.; Clavero, J.; Droguett, D.; Pérez-Martínez, W.; Briceño-De-Urbaneja, I.; Oliva, P. Landslide Susceptibility Using Remote Sensing Data & GIS in a High Andean Area of Central Chile. *IGARSS 2020 - 2020 IEEE International Geoscience and Remote Sensing Symposium, Waikoloa, HI, USA*, **2020**, 6604-6607. doi:10.1109/IGARSS39084.2020.9324317.
19. Intarawichian, N.; Dasananda, S. Analytical Hierarchy Process for Landslide Susceptibility Mapping in Lower Mae Chaem Watershed, Northern Thailand. *Suranaree Journal of Science & Technology* **2010**, *17(3)*, 277-292.

20. Saaty, T.L.; Vargas, L.G. Models, Methods, concepts & applications of the analytic hierarchy process. *In International series in management science/operations research* **2012**. Doi:10.1007/978-1-4614-3597-6.
21. Jenks, G.F; Caspall, F.C. Error on choroplethic maps: definition, measurement, reduction, *Ann. Assoc. Am. Geogr.* **1971**, *61(2)*, 217-244. doi:10.1111/j.1467-8306.1971.tb00779.x.